The scaffold protein JLP plays a key role in regulating ultraviolet B-induced apoptosis in mice

doi: 10.1111/gtc.12135

The scaffold protein JLP plays a key role in regulating ultraviolet B-induced apoptosis in mice

Radnaa Enkhtuya[1], Tokiharu Sato[1], Mitsuo Wakasugi[2], Baljinnyam Tuvshintugs[1], Hirofumi Miyata[1], Takeshi Sakurai[3], Tsukasa Matsunaga[2], Katsuji Yoshioka[1]

[1]Division of Molecular Cell Signaling, Cancer Research Institute, Kanazawa University, Kanazawa 920-1192, Japan

[2]Graduate School of Natural Science and Technology, Kanazawa University, Kanazawa 920-1192, Japan.

[3]Department of Molecular Neuroscience and Integrative Physiology, Faculty of Medicine, Kanazawa University, Kanazawa 920-8640, Japan

Running title: Regulation of UVB-induced apoptosis by JLP

Total character count: 25,482

Corresponding author: Katsuji Yoshioka

Division of Molecular Cell Signaling, Cancer Research Institute, Kanazawa University, Kakuma-machi, Kanazawa, Ishikawa 920-1192, Japan.

Tel: +81-76-234-4532

Fax: +81-76-234-4532

E-mail: katsuji@staff.kanazawa-u.ac.jp.

Abstract

The ultraviolet B (UVB) component of sunlight can cause severe damage to skin cells and even induce skin cancer. Growing evidence indicates that the UVB-induced signaling network is complex and involves diverse cellular processes. In this study we investigated the role of c-Jun NH_2-terminal kinase-associated leucine zipper protein (JLP), a scaffold protein for mitogen-activated protein kinase (MAPK) signaling cascades, in UVB-induced apoptosis. We found that UVB-induced skin epidermal apoptosis was prevented in *Jlp* knockout (KO) as well as in keratinocyte-specific *Jlp* KO mice. Analysis of the repair of UVB-induced DNA damage over time showed no evidence for the involvement of JLP in this process. In contrast, UVB-stimulated p38 MAPK activation in the skin was impaired in both *Jlp* KO and keratinocyte-specific *Jlp* KO mice. Moreover, topical treatment of UVB-irradiated mouse skin with a p38 inhibitor significantly suppressed the epidermal apoptosis in wild-type mice, but not in *Jlp* KO mice. Our findings suggest that JLP in skin basal keratinocytes plays an important role in UVB-induced apoptosis by modulating p38 MAPK signaling pathways. This is the first study to demonstrate a critical role for JLP in an *in vivo* response to environmental stimulation.

Introduction

Skin represents the largest and outermost organ in the human body, and thus, is constantly challenged by various environmental insults. It has been well documented that ultraviolet (UV) exposure is a major risk factor for skin cancer (Bowden, 2004). UVB light (280-320 nm) is mostly absorbed in the epidermis, and induces DNA photolesions, such as cyclobutane pyrimidine dimers (CPD) and (6-4) photoproducts (6-4PP), which, if inefficiently repaired result in deleterious mutations. When DNA damage is too extensive to be repaired, apoptosis is induced. This is a protective mechanism that eliminates damaged and potentially carcinogenic cells. UVB irradiation also induces alterations in gene expression that are mediated by signaling molecules, including mitogen-activated protein kinases (MAPKs) (Bode and Dong, 2003; Bowden, 2004). Growing evidence indicates that the UVB-induced signaling network is complex and involves diverse cellular processes, such as apoptosis and survival. To date, the mechanisms involved in regulating UVB-induced apoptosis pathways remain unclear.

Mammalian MAPK signaling cascades, consisting of MAPK kinase kinase, MAPK kinase, and MAPK, play crucial roles in multiple cellular processes, including cell proliferation, differentiation, and apoptosis (Minden and Karin, 1997; Robinson and Cobb, 1997; Davis, 2000; Kyriakis and Avruch, 2001). Three MAPK subfamilies have been extensively studied: extracellular signal-regulated kinase (ERK), c-Jun NH_2-terminal kinase (JNK), and p38 MAPKs. ERK MAPKs primarily respond to mitogenic and differentiation stimuli, while JNK and p38 MAPKs are strongly activated by inflammatory signals and stress, including UV irradiation. The mammalian MAPK signaling system employs scaffold proteins, in part, to organize the MAPK signaling components into functional modules, thereby enabling the efficient activation of specific MAPK cascades (Morrison and Davis, 2003; Yoshioka, 2004; Dhanasekaran, et al., 2007). To date, nearly 20 proteins have been identified as scaffold factors for mammalian MAPK signaling

pathways. However, the *in vivo* functions of most of these proteins remain largely unknown. JNK-associated leucine zipper protein (JLP), splice variants of which are known as SPAG9 (Shankar et al., 1998) and JIP4 (Kelkar et al., 2005), has been identified as a scaffold protein for JNK and p38 cascades (Lee et al., 2002). We previously reported that JLP-null mice are viable and grow normally, but exhibit reduced male fertility (Iwanaga et al., 2008).

To better understand the complex UVB response, in this study we investigated the function of JLP in UVB-induced apoptosis in the skin by analyzing *Jlp*-deficient mice. Our results suggest that JLP plays an important role in this apoptosis by modulating p38 MAPK signaling cascades.

Results

Phenotypic and histological analysis of *Jlp*$^{-/-}$ mice

We previously generated *Jlp*$^{-/-}$ mice by targeted gene disruption using 129-derived ES cell lines (Iwanaga et al., 2008). Even after extensive backcrossing (more than 10 times) onto the C57BL/6 background, *Jlp*$^{-/-}$ mice exhibited a lightened coat color and pale skin (Fig. 1A), as reported for homozygous *dazzle* mice (Krebs and Beutler, 2010). The *dazzle* mouse was generated by N-ethyl-N-nitrosourea mutagenesis on the C57BL/6 background and contains a missense mutation in the *Jlp* gene (Krebs and Beutler, 2010). Taken together, these results indicate that the pigmentation defects can be attributed to the loss of normal JLP function. However, there were no obvious histological differences observed in the skin among wild-type (*Jlp*$^{+/+}$), control (*Jlp*$^{+/-}$), and *Jlp*$^{-/-}$ mice (Fig. 1B and data not shown).

Jlp-deficient mice exhibit decreased apoptosis in response to UVB irradiation

We next examined the effect of *Jlp* deficiency on UVB-induced apoptosis in mouse skin. To this end, we performed immunohistochemical analysis using an antibody against active caspase-3, a well characterized apoptotic marker. Upon UVB exposure, the number of active caspase-3-positive cells, which were detected mostly in the epidermis (Fig. 2A), was significantly decreased in *Jlp*$^{-/-}$ compared with control mice (Fig. 2B). These results suggested that JLP is a positive regulator of UVB-induced apoptotic pathways.

Effect of *Jlp* deficiency on the repair of UVB-induced DNA damage

To gain insight into the mechanisms underlying the attenuated UVB-induced apoptosis in *Jlp*-deficient mice, we investigated the DNA repair capability of keratinocytes lacking JLP. We examined the repair of 6-4PPs, which, compared to CPDs, are more quickly and effectively excised from UV-irradiated cellular DNA (Mitchell et al., 1985; Mizuno et al.,

1991), and thus are a useful indicator for evaluating DNA repair. We examined the 6-4PP repair over time in epidermal keratinocytes prepared from the control and *Jlp*$^{-/-}$ mice. After UVB exposure, the 6-4PP lesions were removed with similar kinetics in the control and *Jlp*$^{-/-}$ keratinocytes (Fig. 3), suggesting that JLP is not involved in the DNA excision repair of UVB-induced damage, and furthermore that the inhibition of apoptosis observed in *Jlp*$^{-/-}$ mice is not due to a decreased accumulation of DNA damage.

Impaired UVB irradiation-induced MAPK activation in *Jlp*$^{-/-}$ mice

Next, we asked whether JLP ablation perturbs the normal MAPK activation response to UVB irradiation. We analyzed the UVB-induced levels of phosphorylated and activated JNK (p-JNK), p38 (p-p38), and ERK (p-ERK) in the skin of control and *Jlp*$^{-/-}$ mice by Western blotting (Fig. 4A). While the p-ERK levels were similar between the control and *Jlp*$^{-/-}$ mice, modest and substantial decreases in the levels of p-JNK and p-p38, respectively, were observed in the skin samples of *Jlp*$^{-/-}$ mice (Fig. 4A, compare lanes 3 and 4). We further analyzed the UVB-induced p38 activation by immunohistochemistry. As shown in Figure 4B and C, the p-p38 immunopositive signals in the epidermis were significantly lower in *Jlp*$^{-/-}$ mice compared to control mice.

Generation and analysis of mice with a keratinocyte-specific deletion of JLP

To examine whether JLP expressed in skin basal keratinocytes is responsible for UVB-induced apoptosis, we generated keratinocyte-specific *Jlp* conditional KO (cKO) mice by crossing mice carrying *Jlp* loxP-flanked (floxed) alleles with Keratin5-Cre (K5-Cre) transgenic mice. The region-specific expression of Cre recombinase in the K5-Cre mice was confirmed using the *Rosa26-lacZ* reporter (*R26R*) (Fig. S1 in Supporting Information). The loss of JLP expression in keratinocytes was assessed by Western blotting of cell lysates prepared from primary keratinocytes isolated from control (*Jlp*$^{flox/+}$;K5-Cre) and *Jlp* cKO (*Jlp*$^{flox/flox}$;K5-Cre) mice (Fig. 5A). The results indicated

that the *Jlp* gene was successfully disrupted in keratinocytes by K5-Cre-mediated recombination. We then analyzed the UVB-induced apoptosis and p38 MAPK activation in the control and *Jlp* cKO mice. Consistent with the findings in $Jlp^{-/-}$ mice (Fig. 2A, B), the *Jlp* cKO mice exhibited significantly decreased apoptosis in the epidermis in response to UVB irradiation, compared with control mice (Fig. 5B, C). Moreover, reduced levels of p-p38 were observed in the skin samples of *Jlp* cKO mice by Western blotting (Fig. 5D). We also analyzed the UVB-induced p38 activation by immunohistochemistry, and found that the p38 immunosignals in the epidermis were significantly lower in the *Jlp* cKO mice compared with control mice (Fig. 5E, F).

Involvement of p38 signaling in UVB-induced apoptosis

Finally, we investigated whether p38 signaling is required for UVB-induced apoptosis in mouse skin using SB203580, a small molecule inhibitor of p38. As shown in Figure 6, topical treatment of UVB-irradiated mouse skin with the p38 inhibitor significantly reduced the number of active caspase-3-positive cells in the epidermis of wild-type mice, but not *Jlp* KO mice, indicating that p38 signaling plays a pro-apoptotic role in response to UVB exposure.

Discussion

In the present study, we examined the role of JLP in UVB-induced apoptosis in skin epidermal tissues, and found that *Jlp*-deficient mice exhibit a substantially reduced apoptotic response. To our knowledge, this is the first demonstration of a critical role for JLP in an *in vivo* response to environmental stimulation. We also found that conventional *Jlp* KO mice and keratinocyte-specific *Jlp* cKO mice, in which *Jlp* is disrupted in K5-expressing basal cells, exhibit almost identical effects on UVB-induced apoptosis (Figs 2, 4, 5). Thus, the lack of JLP expression in basal keratinocytes is most likely responsible for the decreased susceptibility of the *Jlp* mutant mice to UVB-induced stress.

The UVB-induced activation of p38 MAPK was significantly attenuated in the epidermis of *Jlp* KO and *Jlp* cKO mice (Figs. 4C, 5F). In addition, topical application of a p38 inhibitor to the skin significantly suppressed the UVB-induced apoptosis in wild-type mice, but not in *Jlp* KO mice (Fig. 6). It is therefore likely that JLP functions as a scaffolding factor for pro-apoptotic p38 pathways following UVB stimulation in basal keratinocytes. However, we cannot rule out the possibility that JLP and/or p38 expressed in cells or tissues other than keratinocytes also affects the regulation of the UVB-induced apoptosis independently or cooperatively. At present, the detailed mechanisms underlying UVB-induced JLP-p38 signaling remain unclear. However, considering evidence that UVB exposure stimulates the generation of reactive oxygen species (ROS) (Van Laethem et al., 2009), and that ROS regulate p38 activation (Dolado et al., 2007), UVB-induced ROS may activate JLP-mediated p38 signaling pathways.

JNK/stress-activated protein kinase-associated protein 1 (JSAP1, also known as JIP3 or Sunday Driver), which is highly homologous with JLP in its sequence and domain structure, has been identified as a scaffold protein for JNK signaling pathways (Ito et al., 1999; Kelkar et al., 2000). Recently, Ongusaha et al. (2008) analyzed JSAP1/JIP3 knockdown cultured cells, and reported that Rho-associated kinase 1 plays an essential

role in UVB-induced apoptosis by regulating JSAP1/JIP3-JNK pathways. Thus, upon UVB stimulation, the scaffold proteins JSAP1 and JLP may be responsible for the efficient activation of JNK and p38 signaling pathways, respectively, leading to apoptosis. In addition, it is also possible that JSAP1 and JLP scaffolds are partially redundant in the regulation of JNK and/or p38 signaling pathways in response to UVB irradiation, although to date, no functional redundancy between JSAP1 and JLP has been reported. Future studies, including the analysis of keratinocyte-specific *Jsap1* cKO and *Jsap1* and *Jlp* double cKO mice, will be required to clarify this issue.

Here, we identified the scaffold protein JLP as a novel positive regulator of UVB-induced apoptosis. It will be interesting to determine whether *Jlp*-deficient mice exhibit an increased susceptibility to skin cancers, especially basal cell carcinoma, in response to UVB irradiation. Our *Jlp*-deficient mice may be a useful model for studying apoptosis as well as the development and progression of UVB-induced skin cancer.

Experimental procedures

Mice

All experimental procedures performed with mice were approved by the Institutional Animal Care and Use Committee of Kanazawa University. *Jlp*$^{-/-}$ mice were generated previously (Iwanaga et al., 2008). The generation of mice carrying floxed alleles of *Jlp* will be described elsewhere in detail. Briefly, two loxP sites were inserted to flank exon 5 of the *Jlp* gene. These mutant mice were backcrossed to C57BL/6 for more than ten generations, and the resulting mice were used in this study. C57BL/6 mice were obtained from Japan SLC (Hamamatsu, Japan), K5-Cre transgenic mice (Tarutani et al., 1997) from the Center for Animal Resources and Development of Kumamoto University, and *R26R* mice from the Jackson Laboratory (Bar Harbor, ME, USA).

UVB irradiation and treatment with a pharmacological p38 inhibitor

Adult mice were shaved on the back with hair clippers and an electric shaver under anesthesia. After 24 hours, deeply anesthetized mice were irradiated with UVB at a dose of 2.8 kJ/m^2 using a CL-1000 ultraviolet crosslinker (UVP, Upland, CA, USA). For the topical inhibition of p38 MAPK, SB203580 (#13067; Cayman Chemical, Ann Arbor, MI, USA) was dissolved in acetone and used at a dose of 0.5 μmol. The inhibitor was reconstituted immediately before use and applied in a volume of 40 μL to the dorsal skin for 1 hour before irradiation and immediately following irradiation.

Histological analysis, immunofluorescence, and β-galactosidase staining

Adult mice were deeply anesthetized and fixed by transcardial perfusion with 4% paraformaldehyde (PFA). The back skin was removed, postfixed in 4% PFA, cryoprotected in 30% sucrose, and embedded in Tissue-Tek OCT compound (Sakura Finetek, Tokyo, Japan). Frozen 7-μm sections were subjected to hematoxylin and eosin

staining for histological analysis, and 20-μm frozen sections were subjected to immunohistochemical staining using an anti-active caspase-3 antibody. For phosphorylated and activated p38 (p-p38) immunostaining, back skin was removed from deeply anesthetized mice, embedded in OCT compound, and frozen in liquid nitrogen. Frozen sections (20-μm thick) were fixed in 4% PFA for 10 minutes and subjected to immunohistochemical analysis. *R26R* mice were mated with K5-Cre mice for β-galactosidase staining. Mice at postnatal day (P) 5 were deeply anesthetized, and the back skin was removed, fixed in 4% PFA, cryoprotected in 30% sucrose, and embedded in OCT compound. Frozen sections (20-μm thick) were stained in in PBS containing 1 mg/mL X-gal (5-Bromo-4-Chloro-3-Indolyl-β-D-Galactoside; Takara Bio, Otsu, Japan), 2 mM $MgCl_2$, 5 mM potassium ferrocyanide and 5 mM potassium ferricyanide. Immunohistochemistry was performed as previously described (Sato et al., 2011). The following primary antibodies were used: anti-active caspase-3 antibody (1:600; #9661; Cell Signaling, Boston, MA, USA) and anti-p-p38 antibody (1:1600; #4511; Cell Signaling). Secondary antibodies were Alexa fluor 488- (#A11008) and 568-conjugated (#A11011) antibodies (both diluted at 1:1000; Invitrogen, Rockville, MD, USA). In some experiments, nuclei were stained with 4,6-diamidino-2-phenylindole (DAPI; Sigma, St Louis, MO, USA). Fluorescence images were captured with a confocal laser-scanning microscope (LSM510 META, Carl Zeiss, Oberkochen, Germany). Other images were captured with a fluorescence microscope (BX50, Olympus, Tokyo, Japan).

Western blotting

Back skin was removed from deeply anesthetized mice, snap frozen in liquid nitrogen, pulverized with a mortar and pestle, and lysed in RIPA buffer (50 mM Tris-HCl pH 7.4, 150 mM NaCl, 1% Nonidet P40, 0.1% sodium deoxycholate) containing Protease Inhibitor Cocktail (Sigma). Primary keratinocytes were also lysed in the same buffer. Western blotting analysis was performed as previously described (Sato et al., 2008), using

anti-JLP (Iwanaga et al., 2008; Gantulga et al., 2008) (2 μg ml^{-1}), anti-p-JNK (#9251), anti-pan-JNK (#9258), anti-p-p38 (#4631), anti-pan-p38 (#9212), anti-p-ERK (#4377), anti-pan-ERK (#9102) (all diluted at 1:1000; Cell Signaling), and anti-α-tubulin (1:5000; #T5168; Sigma) antibodies. Proteins were visualized with the Immobilon Western Chemiluminescence HRP Substrate (Millipore, Billerica, MA, USA).

Primary keratinocytes

Primary mouse keratinocytes were prepared from newborn mice as previously described (Zhang et al., 2012), and cultured in CnT-57 medium (CELLnTEC, Berne, Switzerland) at 37˚C and 5% CO_2. Subconfluent passage 1 cells were used for experiments.

Measurement of 6-4PP repair

Appropriate numbers of keratinocytes from $Jlp^{+/-}$ or $Jlp^{-/-}$ mice were plated in 35-mm glass-bottom dishes, and then UVB-induced 6-4PP lesions were measured as previously described (Wakasugi et al., 2009), using the 6-4PP-specific antibody, 64M-5 (Mori et al., 1991). Immunofluorescence images of labeled 6-4PP lesions were obtained using the All-in-One fluorescence microscope BZ-9000 (Keyence, Osaka, Japan), and 6-4PP levels were calculated from the fluorescence intensities measured using ImageJ software (National Institutes of Health, Bethesda, MD, USA).

Statistical analysis

Significance was determined using the two-tailed unpaired Student's *t*-test. Values of $P < 0.05$ were considered to be statistically significant.

Acknowledgements

This work was supported in part by Grants-in-Aid from the Ministry of Education, Culture, Sports, Science and Technology of Japan.

References

Bode, A.M. & Dong, Z. (2003) Mitogen-activated protein kinase activation in UV-induced signal transduction. *Sci. STKE* **2003**, RE2.

Bowden, G.T. (2004) Prevention of non-melanoma skin cancer by targeting ultraviolet-B-light signalling. *Nat. Rev. Cancer* **4**, 23-35.

Davis, R.J. (2000) Signal transduction by the JNK group of MAP kinases. *Cell* **103**, 239-252.

Dhanasekaran, D.N., Kashef, K., Lee, C.M., Xu, H. & Reddy, E.P. (2007) Scaffold proteins of MAP-kinase modules. *Oncogene* **26**, 3185-3202.

Dolado, I., Swat, A., Ajenjo, N., De Vita, G., Cuadrado, A. & Nebreda, A.R. (2007) p38alpha MAP kinase as a sensor of reactive oxygen species in tumorigenesis. *Cancer Cell* **11**, 191-205.

Gantulga, D., Tuvshintugs, B., Endo, Y., Takino, T., Sato, H., Murakami, S. & Yoshioka, K. (2008) The scaffold protein c-Jun NH_2-terminal kinase-associated leucine zipper protein regulates cell migration through interaction with the G protein G(alpha 13). *J. Biochem.* **144**, 693-700.

Ito, M., Yoshioka, K., Akechi, M., Yamashita, S., Takamatsu, N., Sugiyama, K., Hibi, M., Nakabeppu, Y., Shiba, T. & Yamamoto, K. (1999) JSAP1, a novel Jun N-terminal protein kinase (JNK) that functions as scaffold factor in the JNK signaling pathway. *Mol. Cell. Biol.* **19**, 7539-7548.

Iwanaga, A., Wang, G., Gantulga, D., Sato, T., Baljinnyam, T., Shimizu, K., Takumi, K., Hayashi, M., Akashi, T., Fuse, H., Sugihara, K., Asano, M. & Yoshioka, K. (2008) Ablation of the scaffold protein JLP causes reduced fertility in male mice. *Transgenic Res.* **17**, 1045-1058.

Kelkar, N., Gupta, S., Dickens, M. & Davis, R.J. (2000) Interaction of a mitogen-activated protein kinase signaling module with the neuronal protein JIP3. *Mol. Cell. Biol.* **20**,

1030-1043.

Kelkar, N., Standen, C.L. & Davis, R.J. (2005) Role of the JIP4 scaffold protein in the regulation of mitogen-activated protein kinase signaling pathways. *Mol. Cell. Biol.* **25**, 2733-2743.

Krebs, P. & Beutler, B. (2010) Dazzle is an allele of Spag9 and results in pigmentation and sperm defects. MGI Direct Data Submission [MGI Ref ID J:159363] Available from URL: http://www.informatics.jax.org/reference/J:159363.

Kyriakis, J.M. & Avruch J. (2001) Mammalian mitogen-activated protein kinase signal transduction pathways activated by stress and inflammation. *Physiol. Rev.* **81**, 807-869.

Lee, C.M., Onésime, D., Reddy, C.D., Dhanasekaran, N. & Reddy, E.P. (2002) JLP: A scaffolding protein that tethers JNK/p38MAPK signaling modules and transcription factors. *Proc. Natl. Acad. Sci. USA* **99**, 14189-14194.

Minden, A. & Karin, M. (1997) Regulation and function of the JNK subgroup of MAP kinases. *Biochim. Biophys. Acta* **1333**, F85-104.

Mitchell, D.L., Haipek, C.A. & Clarkson, J.M. (1985) (6-4) photoproducts are removed from the DNA of UV-irradiated mammalian cells more efficiently than cyclobutane pyrimidine dimers. *Mutat. Res.* **143**, 109-112.

Mizuno, T., Matsunaga, T., Ihara, M. & Nikaido, O. (1991) Establishment of a monoclonal antibody recognizing cyclobutane-type thymine dimers in DNA: a comparative study with 64M-1 antibody specific for (6-4) photoproducts. *Mutat. Res.* **254**, 175-184.

Mori, T., Nakane, M., Hattori, T., Matsunaga, T., Ihara, M. & Nikaido, O. (1991) Simultaneous establishment of monoclonal antibodies specific for either cyclobutane pyrimidine dimer or (6-4) photoproduct from the same mouse immunized with ultraviolet-irradiated DNA. *Photochem. Photobiol.* **54**, 225-232.

Morrison, D.K. & Davis, R.J. (2003) Regulation of MAP kinase signaling modules by

scaffold proteins in mammals. *Annu. Rev. Cell Dev. Biol.* **19**, 91-118.

Ongusaha, P.P., Qi, H.H. & Raj, L. (2008) Identification of ROCK1 as an upstream activator of the JIP-3 to JNK signaling axis in response to UVB damage. *Sci. Signal* **1**, ra14.

Robinson, M.J. & Cobb, M.H. (1997) Mitogen-activated protein kinase pathways. *Curr. Opin. Cell Biol.* **9**, 180-186.

Sato, T., Torashima, T., Sugihara, K., Hirai, H., Asano, M. & Yoshioka, K. (2008) The scaffold protein JSAP1 regulates proliferation and differentiation of cerebellar granule cell precursors by modulating JNK signaling. *Mol. Cell. Neurosci.* **39**, 569-578.

Sato, T., Enkhbat, A. & Yoshioka, K. (2011) Role of plasma membrane localization of the scaffold protein JSAP1 during differentiation of cerebellar granule cell precursors. *Genes Cells* **16**, 58-68.

Shankar, S., Mohapatra, B. & Suri, A. (1998) Cloning of a novel human testis mRNA specifically expressed in testicular haploid germ cells, having unique palindromic sequences and encoding a leucine zipper dimerization motif. *Biochem. Biophys. Res. Commun.* **243**, 561-565.

Tarutani, M., Itami, S., Okabe, M., Ikawa, M., Tezuka, T., Yoshikawa, K., Kinoshita, T. & Takeda, J. (1997) Tissue-specific knockout of the mouse Pig-a gene reveals important roles for GPI-anchored proteins in skin development. *Proc. Natl. Acad. Sci. USA* **94**, 7400-7405.

Van Laethem, A., Garmyn, M. & Agostinis, P. (2009) Starting and propagating apoptotic signals in UVB irradiated keratinocytes. *Photochem. Photobiol. Sci.* **8**, 299-308.

Wakasugi, M., Kasashima, H., Fukase, Y., Imura, M., Imai, R., Yamada, S., Cleaver, J.E. & Matsunaga, T. (2009) Physical and functional interaction between DDB and XPA in nucleotide excision repair. *Nucleic Acids Res.* **37**, 516-525.

Yoshioka, K. (2004) Scaffold proteins in mammalian MAP kinase cascades. *J. Biochem.*

135, 657-661.

Zhang, L.J., Bhattacharya, S., Leid, M., Ganguli-Indra, G. & Indra, A.K. (2012) Ctip2 is a dynamic regulator of epidermal proliferation and differentiation by integrating EGFR and Notch signaling. *J. Cell Sci.* **125**, 5733-5744.

Figure legends

Figure 1. Phenotypic and histological analysis of *Jlp*$^{-/-}$ mice. (A) Macroscopic appearance of control (*Jlp*$^{+/-}$) and *Jlp*$^{-/-}$ adult mice. (B) Hematoxylin and eosin staining of 7-μm-thick frozen sections from the shaved back skin of control and *Jlp*$^{-/-}$ adult mice. The images were captured by an Olympus BX50 microscope with a 20x objective. E, epidermis; D, dermis; HF, hair follicle. Scale bar, 100 μm.

Figure 2. JLP ablation reduces UVB-induced apoptosis in mice. (A) Immunohistochemical staining for active caspase-3 in control (*Jlp*$^{+/-}$) and *Jlp*$^{-/-}$ mice. The backs of control and *Jlp*$^{-/-}$ adult mice were shaved and irradiated with 2.8 kJ/m^2 of UVB. After 24 hours, skin samples were obtained and fixed, and 20-μm-thick frozen sections were stained with an anti-active caspase-3 antibody and DAPI. The images were captured by a Zeiss LSM510 META confocal microscope with a 20x objective. Scale bar, 100 μm. (B) Quantification of the results in **A**. The number of active caspase-3-positive cells in the epidermis was counted over a linear distance of 20-30 mm, and averaged for each 1-mm interval. Values are the mean ± SEM from three independent experiments. ***$P < 0.001$.

Figure 3. Kinetics of 6-4PP repair in *Jlp*$^{-/-}$ keratinocytes. Primary keratinocytes derived from control (*Jlp*$^{+/-}$) and *Jlp*$^{-/-}$ P0 mice were irradiated with 160 J/m^2 of UVB. The cells were incubated for the indicated periods and processed for the detection of 6-4PP. Each point represents the mean ± SEM from three independent experiments.

Figure 4. Impaired MAPK activation in the skin of *Jlp*$^{-/-}$ mice following UVB irradiation. (A) Western blotting analysis of MAPK activation in the skin of control (*Jlp*$^{+/-}$) and *Jlp*$^{-/-}$ mice following UVB exposure. The backs of control and *Jlp*$^{-/-}$ adult mice were shaved and treated with (UVB(+)) or without (UVB(-)) 2.8 kJ/m^2 of UVB, as indicated. Thirty

minutes after irradiation, cell lysates were prepared from the skin samples, and analyzed by Western blotting (50 μg lysate/lane) with the indicated antibodies. α-tubulin was used as a loading control. (B) Immunohistochemical staining for p-p38 in control ($Jlp^{+/-}$) and $Jlp^{-/-}$ mice. Control and $Jlp^{-/-}$ adult mice were shaved and treated with or without UVB as in **A**. Thirty minutes after irradiation, skin samples were obtained and fixed, and 20-μm-thick frozen sections were stained with anti-p-p38 antibody and DAPI. The images were captured by a Zeiss LSM510 META confocal microscope with a 40x objective. Scale bar, 50 μm. (C) Quantification of the results in **B**. The immunofluorescence signal intensity of p-p38 in the epidermal compartment (approximately 0.2 mm^2) was quantified using ImageJ. The mean intensity per area of the untreated $Jlp^{-/-}$, the irradiated control ($Jlp^{+/-}$), and the irradiated $Jlp^{-/-}$ mice was normalized to the mean intensity per area of the untreated control ($Jlp^{+/-}$) mice, respectively. Values are the mean ± SEM from three independent experiments. n.s., not significant; $^{**}P < 0.01$.

Figure 5. Reduced apoptosis and impaired p38 activation in the skin of keratin-specific *Jlp* cKO mice treated with UVB irradiation. (A) Western blotting analysis of JLP in primary keratinocytes derived from control ($Jlp^{flox/+}$;K5-cre) and *Jlp* cKO ($Jlp^{flox/flox}$;K5-cre) mice. α-tubulin was used as a loading control. (B) Immunohistochemical staining for active caspase-3 in control and *Jlp* cKO mice. Control and *Jlp* cKO adult mice were shaved and irradiated with UVB, and skin specimens were subjected to immunohistochemistry as in Fig. 2A. Scale bar, 100 μm. (C) Quantification of the results in **B** was performed as in Fig. 2B. Values are the mean ± SEM from three independent experiments. $^{*}P < 0.05$. (D) Western blotting analysis of p38 activation in the skin of control and *Jlp* cKO mice in response to UVB exposure. Control and *Jlp* cKO adult mice were shaved and treated with or without UVB as indicated, and cell lysates prepared from the skin samples were subjected to Western blotting as in Fig. 4A. α-tubulin was used as a loading control. (E) Immunohistochemical staining for p-p38 in control and

Jlp cKO mice. Control and *Jlp* cKO adult mice were shaved and treated with or without UVB, and skin specimens were subjected to immunohistochemistry as in Fig. 4B. Scale bar, 50 μm. (F) Quantification of the results in **E** was performed as in Fig. 4C. Values are the mean ± SEM from three independent experiments. n.s., not significant; **P* < 0.05.

Figure 6. Involvement of p38 signaling in UVB-induced apoptosis. Immunohistochemical staining for active caspase-3 in wild-type mice (A) and *Jlp* KO mice (C). The backs of adult mice were shaved and topically treated with 40 μL of either vehicle or SB203580 (0.5 μmol) 1 hour before and just after UVB irradiation at a dose of 2.8 kJ/m^2. After 24 hours, skin specimens were subjected to immunohistochemistry as in Fig. 2A. Scale bar, 100 μm. The results in **A** and **C** were quantified in **B** and **D**, respectively. The number of active caspase-3-positive cells in the epidermis was counted over a linear distance of 10 mm, and averaged for each 1-mm interval. Values are the mean ± SEM from three independent experiments. n.s., not significant; ****P* < 0.001.

Supporting Information

Figure S1. X-gal staining of skin sections from *R26R* and *R26R*;K5-Cre mice. Frozen sections (20-μm-thick) from the back skin of *R26R* and *R26R*;K5-Cre P5 mice were stained in X-gal solution for 24 hours at 37˚C. Dotted lines indicate the border between epidermis and dermis, and arrowheads point to hair follicles. Scale bar, 30 μm.

A

B

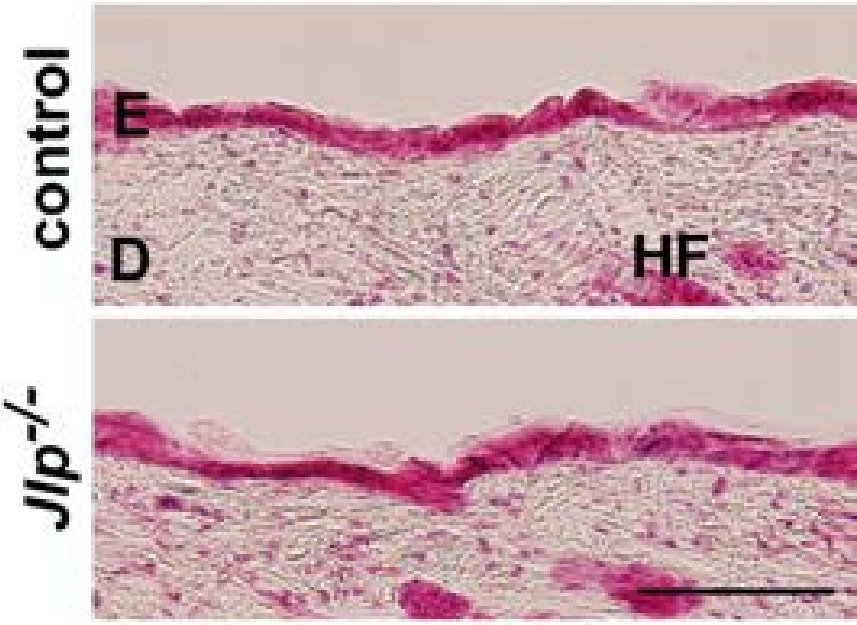

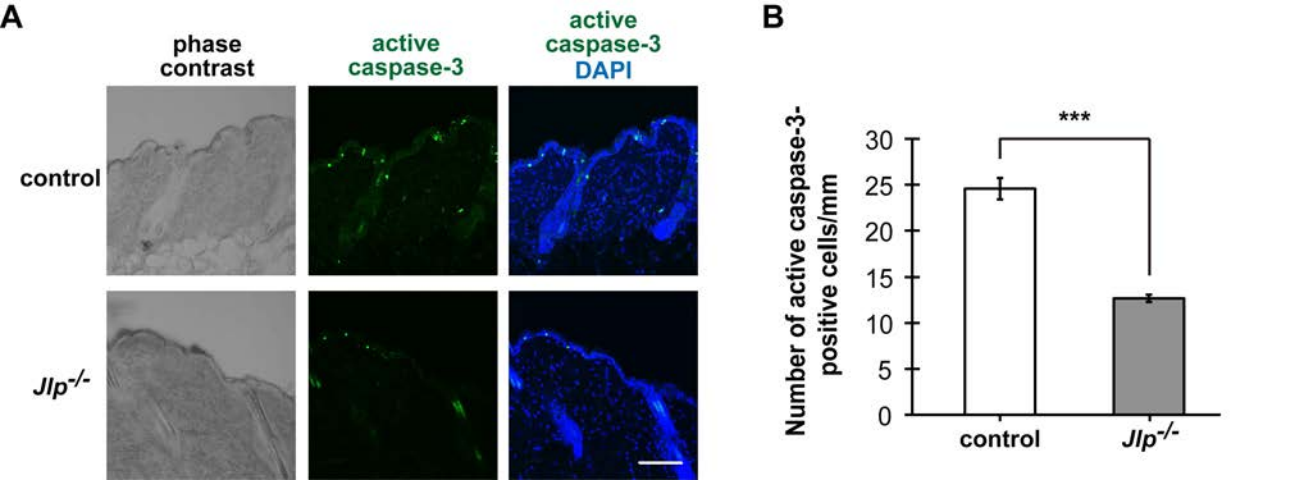
A
phase contrast
active caspase-3
active caspase-3 DAPI
control
Jlp-/-
B
Number of active caspase-3-positive cells/mm
***
30
25
20
15
10
5
0
control
Jlp-/-

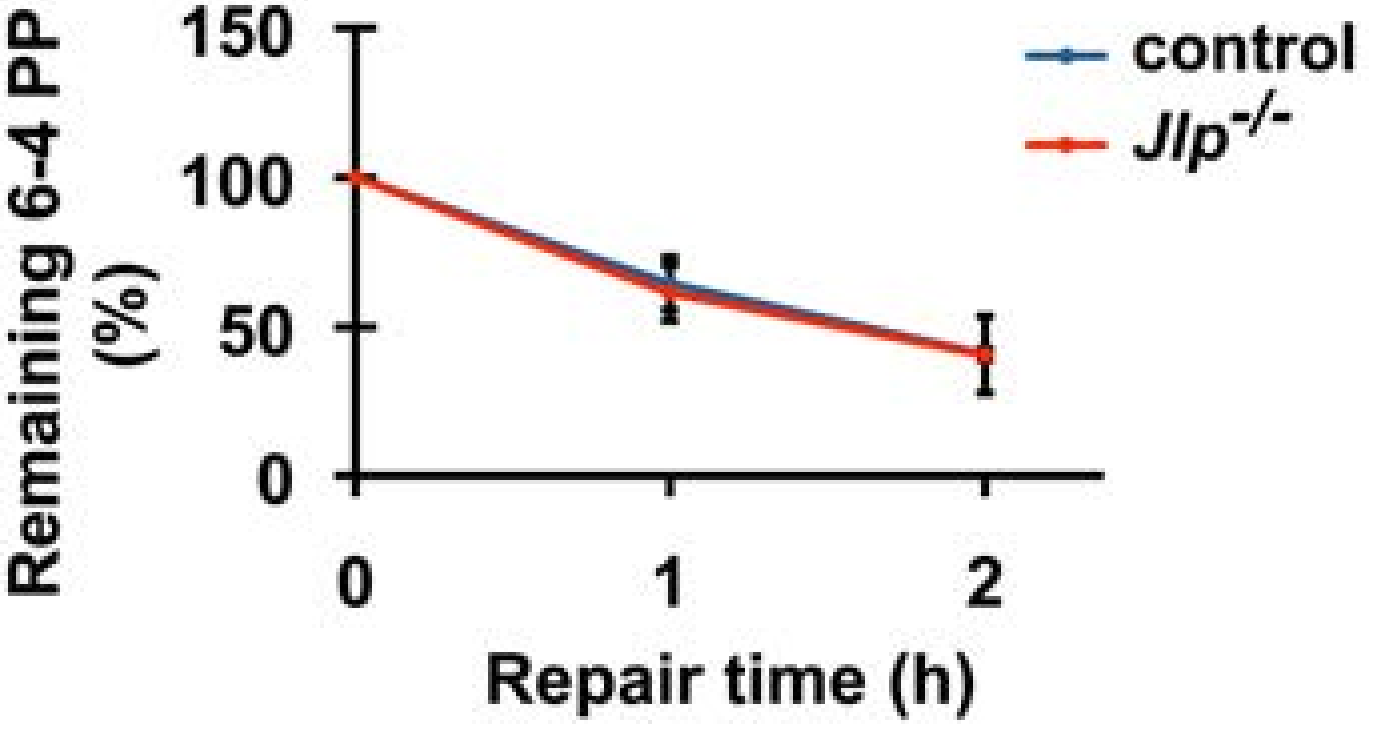
Remaining 6-4 PP (%)
150
100
50
0
0
1
2
Repair time (h)
control
Jlp-/-

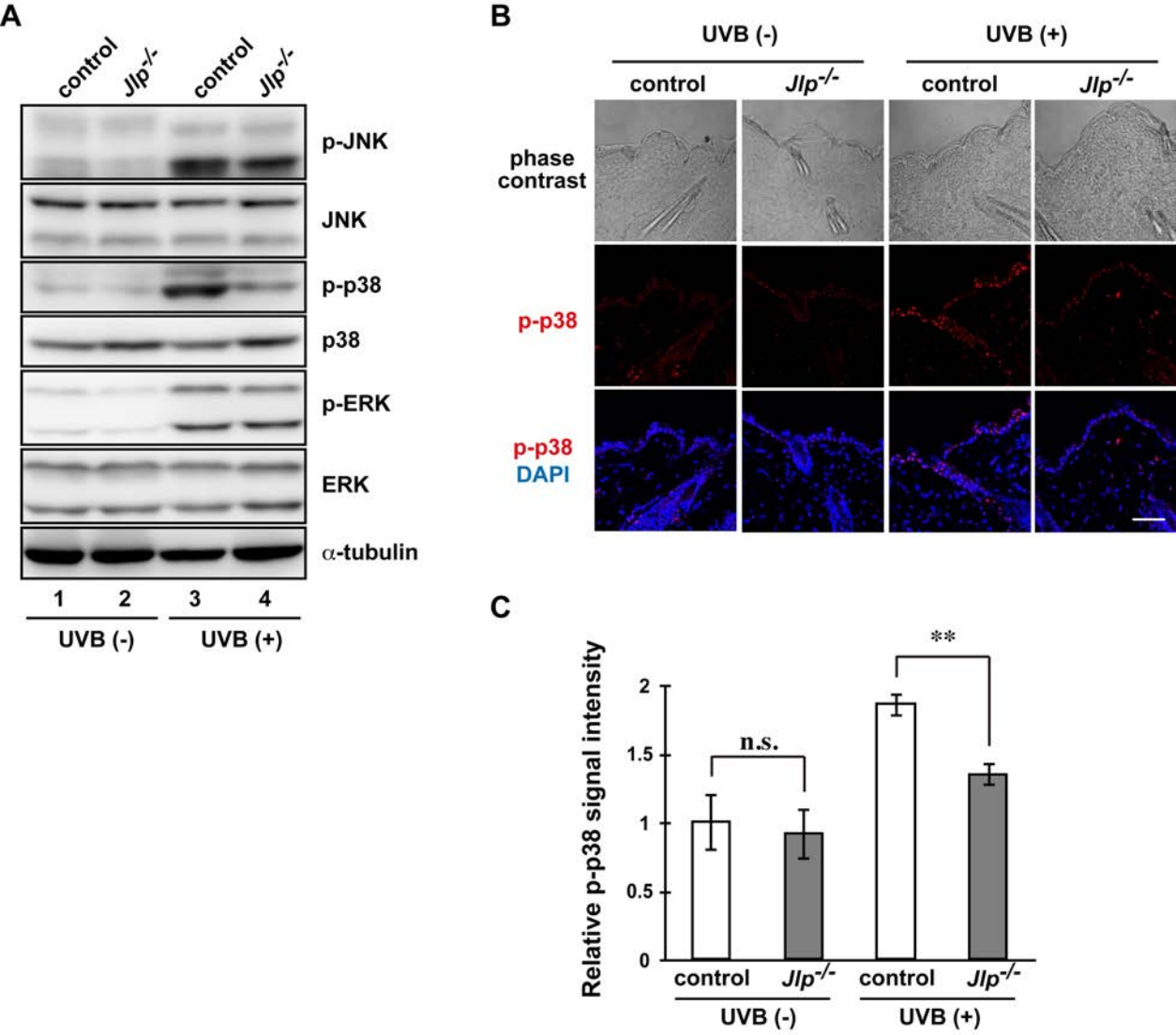
A
control
Jlp-/-
control
Jlp-/-
p-JNK
JNK
p-p38
p38
p-ERK
ERK
α-tubulin
1
2
3
4
UVB (-)
UVB (+)
B
UVB (-)
UVB (+)
control
Jlp-/-
control
Jlp-/-
phase contrast
p-p38
p-p38
DAPI
C
Relative p-p38 signal intensity
2
1.5
1
0.5
0
n.s.
**
control
Jlp-/-
control
Jlp-/-
UVB (-)
UVB (+)

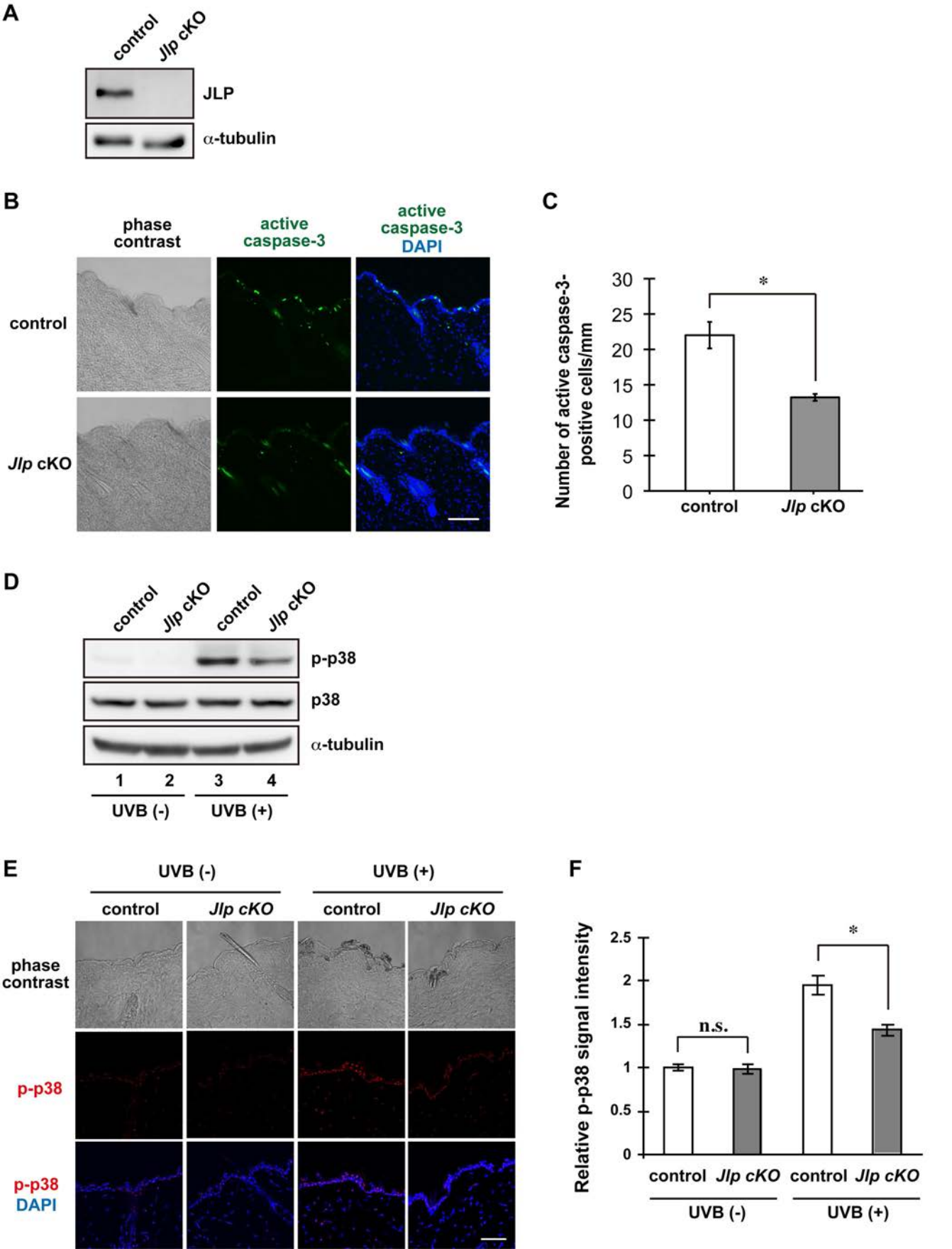
A
control
Jlp cKO
JLP
α-tubulin
B
phase contrast
active caspase-3
active caspase-3 DAPI
control
Jlp cKO
C
Number of active caspase-3-positive cells/mm
30
25
20
15
10
5
0
*
control
Jlp cKO
D
control
Jlp cKO
control
Jlp cKO
p-p38
p38
α-tubulin
1
2
3
4
UVB (-)
UVB (+)
E
UVB (-)
UVB (+)
control
Jlp cKO
control
Jlp cKO
phase contrast
p-p38
p-p38 DAPI
F
Relative p-p38 signal intensity
2.5
2
1.5
1
0.5
0
n.s.
*
control
Jlp cKO
control
Jlp cKO
UVB (-)
UVB (+)

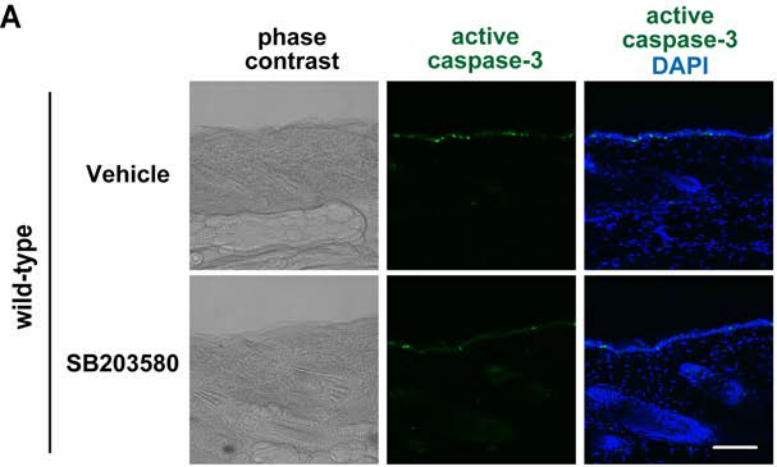
A
phase contrast
active caspase-3
active caspase-3 DAPI
wild-type
Vehicle
SB203580

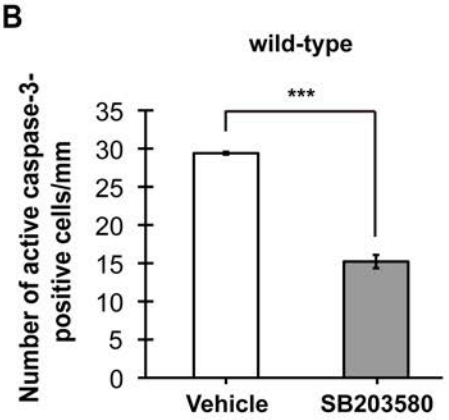
B
wild-type
***
Number of active caspase-3-positive cells/mm
35
30
25
20
15
10
5
0
Vehicle
SB203580

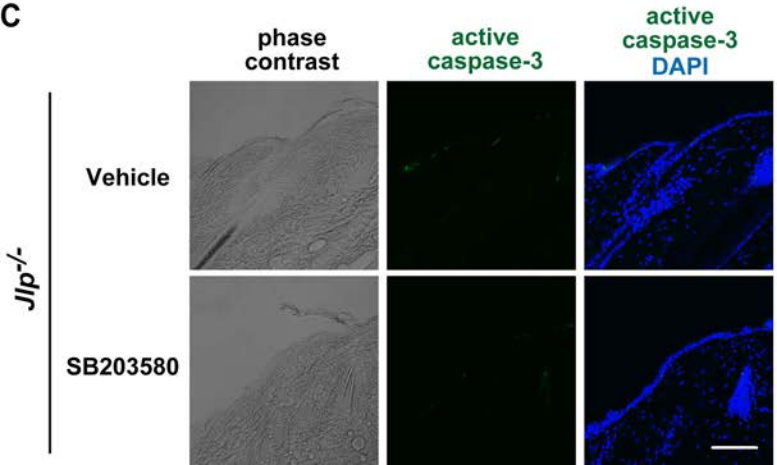
C
phase contrast
active caspase-3
active caspase-3 DAPI
Jlp-/-
Vehicle
SB203580

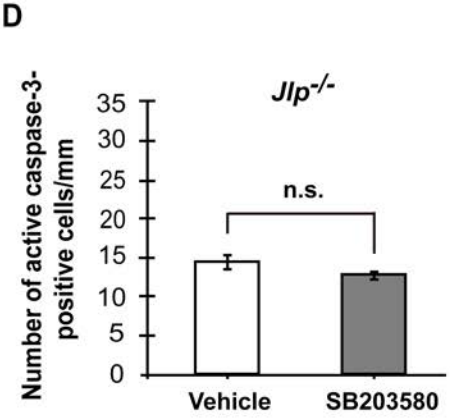
D
Jlp-/-
n.s.
Number of active caspase-3-positive cells/mm
35
30
25
20
15
10
5
0
Vehicle
SB203580

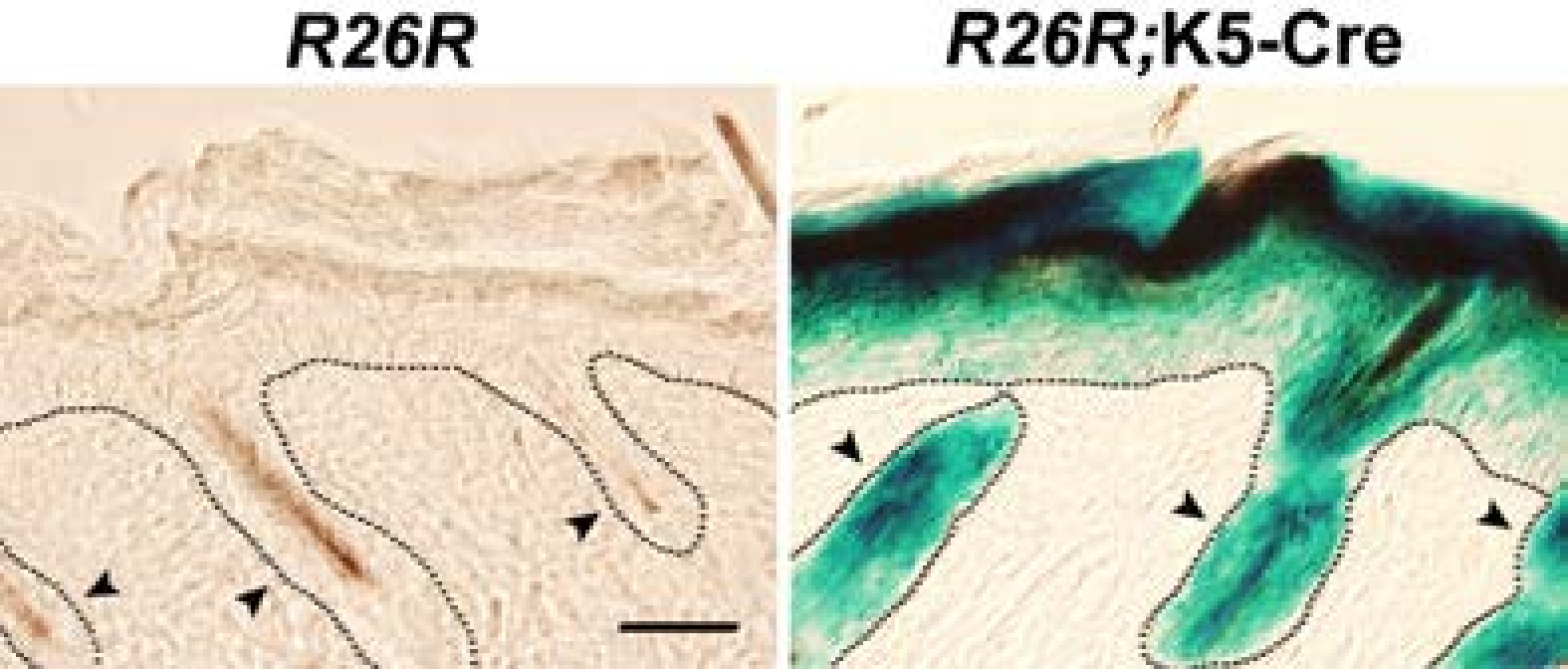
R26R
R26R;K5-Cre